A Metapopulation Model with Explicit Local Population Dynamics

Zhilan Feng
Department of Mathematics, Purdue University,
West Lafayette, IN 47907, USA,
e-mail: zfeng@math.purdue.edu
Robert Swihart
Department of Forestry and Natural Resources,
Purdue University,
West Lafayette, IN 47907, USA,
email: rswihart@fnr.purdue.edu
Yingfei Yi
School of Mathematics,
Georgia Institute of Technology,
Atlanta, GA 30332, USA,
e-mail: yi@math.gatech.edu
Huaiping Zhu
Department of Mathematics and Statistics,
York University, Toronto,
ON, Canada, M3J 1P3,
e-mail: huaiping@mathstat.yorku.ca

July 19, 2003

Abstract

Many patch-based metapopulation models assume that the local population within each patch is at its equilibrium and independent of changes in patch occupancy. We studied a metapopulation model that explicitly incorporates the local population dynamics of two competing species. The singular perturbation method is used to separate the fast dynamics of the local competition and the slow process of patch colonization and extinction. Our results show that the coupled system leads to much more complex outcomes than simple patch models that do not include explicit local dynamics. We also discuss implications of the model for ecological systems in fragmented landscapes.

Keywords: Metapopulation model – fast-slow dynamics – local competition – coexistence

1 Introduction

Destruction and fragmentation of native habitats are widespread and viewed as the most important threats to biodiversity worldwide (Wilcox and Murphy [31]). Agriculture, urban sprawl, deforestation, and other human activities change the composition and physiognomy of landscapes, often altering individual behavior (Sheperd and Swihart [24]; Zollner [33]), population dynamics (Hanski [5]), genetic structure (Gaines *et al.* [4]), and community composition (Wright *et al.* [32]) of organisms. Metapopulation models have been used extensively to study the conservation implications of habitat loss and fragmentation. A metapopulation consists of a set of discrete local populations with independent internal dynamics that are linked by dispersal (Hanski [5]). Metapopulations exist within a network of idealized habitat patches (fragments), occupying some proportion p of these. The original single-species metapopulation model of Levins [13]) assumed that changes in patch occupancy were functions solely of colonization rates of empty patches (c) and extinction rates of occupied patches (e). Although overly simplistic, the Levins model provided an essential framework for studies of spatially structured subpopulation linked by dispersal.

In addition to habitat destruction and fragmentation, interspecific competition can be a powerful force structuring local communities (Hopf *et al.* [11]; McIntosh [15]; Schoener [23]). The joint effects of these forces on community structure is of considerable interest, because asymmetric effects of habitat destruction and fragmentation acting on species have the potential to alter outcomes of interactions for competing species. Theoretical models of various types predict that habitat fragmentation may promote coexistence of competing species by permitting inferior competitors to escape spatially by virtue of greater dispersal ability (Holmes and Wilson [10]; Moilanen and Hanski [16]; Nee and May [17]).

Unfortunately, metapopulation models generalized to multiple species (e.g., Swihart *et al.* [26]; Taneyhill [28]; Wang *et al.* [29]) have failed to incorporate explicitly the local dynamics of species in each patch. An important exception was the model of Hanski and Zhang [7], in which local and metapopulation dynamics were explicitly coupled to enable examination of the effect of migration on metapopulation persistence. They demonstrated that the use of coupled models can provide insights into conditions for metapopulation persistence which cannot be obtained from simple patch models. In this paper, we generalize the model of Hanski and Zhang [7] by including the local dynamics of two weakly competing species. Since local dynamics occur on a much faster time scale than changes in patch occupancy, we can use a singular perturbation argument to separate the model dynamics into two time scales. Our analyses of the slow system show that it is possible for the system to have multiple interior equilibria as well as a unique global interior attractor. When multiple interior equilibria are present, bi-stability may occur, in which case the competing species may stabilize either at an interior equilibrium

(both species stably coexist) or at a boundary equilibrium (one species excludes the other species). Finally, we apply the model to a competitive interaction in a fragmented agroecosystem and discuss the implications of our findings for community structure and species conservation.

2 The model and its fast and slow dynamics

The Levins model has the form

$$\frac{dp}{dt} = cp(1-p) - ep, \tag{2.1}$$

where p denotes the proportion of the occupied patches. Its focus is on extinction e and colonization c rates, with no consideration given to the effect of migration on local dynamics. Such an omission may be reasonable when migration rate is low, but if migration rate is high, failure to consider local dynamics may produce models that predict biased results (Hanski [6]). To study the population-level consequences of local dynamics when migration rates are high Hanksi and Zhang [7] proposed the following patch-based metapopulation model:

$$\begin{cases} \dfrac{dN}{dt} &= rN\left(1-\dfrac{N}{K}\right) - mN + \alpha mNp, \\ \dfrac{dp}{dt} &= \beta\alpha mNp(1-p) - ep, \end{cases} \tag{2.2}$$

where $p \in [0,1]$ is the fraction of the occupied habitat patches, $N \in [0,\infty)$ is the average size of existing local populations, $r > 0$ is the average per capita growth rate due to local births and deaths, $K > 0$ is the average per-patch carrying capacity, $m > 0$ is the per capita emigration rate, $\alpha > 0$ is the fraction of migrating individuals that survived and reached a new patch, $\beta > 0$ is the per capita rate at which a new local population is created in an empty patch by arriving individuals, and $e > 0$ is the extinction rate of local populations. This model assumes different time scales for local and metapopulation dynamics and a uniform size for local populations. The model (2.2) predicts alternative stable equilibria for parameters in a certain range, and qualitatively different model behaviors are possible when the migration parameter, m, varies. Hanksi and Zhang [7] also considered fugitive co-existence by studying an asymmetric competition model in which one competitor is superior (i.e., the inferior species cannot colonize patches occupied by the superior species, and the two competing species cannot co-exist in the same patch).

We generalize the model (Hanksi and Zhang [7]) by incorporating two competing species, each of which can colonize patches occupied by the other species and both of which can co-exist in the same patch. Let N_1 and N_2 denote the number of the species 1 and 2, respectively, and, let p_1 and p_2 denote the fractions of the patches occupied by species 1 and 2, respectively. Assuming competition of the Lotka-Volterra type and

using the subscript i to represent the species i, $i = 1, 2$, we can write the generalized model as follows:

$$\begin{cases} \dfrac{dN_i}{dt} &= r_i N_i \left(1 - \dfrac{N_i}{K_i} - a_{ij}\dfrac{N_j}{K_i}\right) - m_i N_i + \alpha_i m_i N_i p_i, \\ \dfrac{dp_i}{dt} &= \beta_i \alpha_i m_i N_i p_i (1 - p_i) - e_i p_i, \end{cases} \tag{2.3}$$

$i, j = 1, 2,\ i \neq j$. a_{ij} is the competition coefficient expressing the per capita effect of species j on growth rate of species i, and all other parameters are as defined for the model (Hanski and Zhang [7]).

As done by Hanski and Zhang [7], we assume that the changes in patch occupancy occur on a slower time scale than the local population dynamics. Hence, the parameters β_i (patch creation) and e_i (patch extinction), $i = 1, 2$, are much smaller than all other parameters. Assume that

$$\beta_i = \varepsilon\hat{\beta}_i, \quad e_i = \varepsilon\hat{e}_i, \quad i = 1, 2,$$

where $\varepsilon > 0$ is small. Then system (2.3) can be rewritten as

$$\begin{cases} \dfrac{dN_i}{dt} &= N_i F_i(N, p_i), \\ \dfrac{dp_i}{dt} &= \varepsilon p_i G_i(N, p_i), \end{cases} \qquad i = 1, 2, \tag{2.4}$$

where $N = (N_1, N_2)$, and

$$\begin{aligned} F_i(N, p_i) &= r_i \left(1 - \frac{N_i}{K_i} - a_{ij}\frac{N_j}{K_i}\right) - m_i + \alpha_i m_i p_i, \\ G_i(N, p_i) &= \hat{\beta}_i \alpha_i m_i N_i (1 - p_i) - \hat{e}_i, \end{aligned}$$

$i, j = 1, 2,\ \ i \neq j$. The fast dynamics of (2.4) are given by

$$\frac{dN_i}{dt} = N_i F_i(N, p_i), \qquad i = 1, 2. \tag{2.5}$$

In the fast system (2.5), p_1 and p_2 are considered as parameters and will be determined later by the slow system. To make the impact of local dynamics transparent, we consider only the scenario in which coexistence of the two species is possible, for which we make the the following assumptions:

$$a_{12}a_{21} < 1, \qquad \delta_i K_i - a_{ij}\delta_j K_j > 0, \qquad i, j = 1, 2,\ i \neq j, \tag{2.6}$$

where $\delta_i = 1 - (1 - \alpha_i p_i)\frac{m_i}{r_i}$, $i = 1, 2$. Setting the right hand side of (2.5) equal to zero, we obtain a unique positive equilibrium $E^* = (N_1^*, N_2^*)$ (a two-dimensional critical manifold, or slow manifold) described by:

$$\begin{aligned} N_i^* &= \frac{1}{1 - a_{12}a_{21}} \left[K_i \left(1 - \frac{m_i}{r_i}(1 - \alpha_i p_i)\right) \right. \\ &\qquad \left. - a_{ij} K_j \left(1 - \frac{m_j}{r_j}(1 - \alpha_j p_j)\right)\right], \end{aligned} \tag{2.7}$$

$i, j = 1, 2,\ i \neq j$. Note that $N_i^* > 0$ under the condition (2.6). Let $J(E^*)$ denote the Jacobian at E^*, then

$$\det(J(E^*)) = (1 - a_{12}a_{21})\frac{r_1 r_2 N_1^* N_2^*}{K_1 K_2} > 0,$$

as $a_{12}a_{21} < 1$ and $N_i^* > 0$, $i = 1, 2$. It follows that E^* is locally asymptotically stable when it exists. Hence, on the fast time scale, all solutions of (2.3) are hyperbolically asymptotic to the equilibrium E^*, and (2.7) defines a two-dimensional slow manifold. Rescaling the time by letting $\tau = t/\varepsilon$ we obtain the following system which governs the slow dynamics:

$$\frac{dp_i}{d\tau} = p_i\left(\hat{\beta}_i\alpha_i m_i N_i^*(1 - p_i) - \hat{e}_i\right), \qquad i = 1, 2, \tag{2.8}$$

where N_i^* is a function of both p_1 and p_2 (see (2.7)).

We next focus on the slow dynamics. The trivial (extinction) equilibrium, $Q_0 = (p_{10}, p_{20}) = (0, 0)$, always exists. The stability of Q_0 is determined by the relative magnitudes of the patch extinction rate, e_i, and the modified patch colonization rate, c_i:

$$c_i = \frac{\beta_i\alpha_i m_i}{1 - a_{ij}a_{ji}}\left(\big(1 - \frac{m_i}{r_i}\big)K_i - a_{ij}\big(1 - \frac{m_j}{r_j}\big)K_j\right), \tag{2.9}$$

$i, j = 1, 2,\ i \neq j$. Let

$$\lambda_i = \frac{c_i}{e_i}, \qquad i = 1, 2. \tag{2.10}$$

Then, Q_0 is stable if

$$\lambda_i < 1, \qquad i = 1, 2, \tag{2.11}$$

and it is unstable if

$$\lambda_1 > 1 \qquad \text{or} \qquad \lambda_2 > 1. \tag{2.12}$$

In the standard Lotka-Volterra competition model, or in metapopulation competition models that do not explicitly incorporate local population dynamics (Slatkin [25]; Taneyhill [28]; Wang *et al.* [29]), no stable non-trivial equilibria can exist when the trivial equilibrium is stable. Hence, the two species cannot stably coexist if the extinction equilibrium is stable. This is not the case in our model. For example, (2.8) may have a stable interior (coexistence) equilibrium even when the parameters satisfy $\lambda_i < 1$, $i = 1, 2$, which is the stability condition for the trivial equilibrium. In fact, the system (2.8) may have as many as nine equilibria, as shown in Figure 1.

The additional condition (besides $\lambda_i < 1,\ i = 1, 2$) that excludes the existence of an interior equilibrium is that at least one of the following two inequalities holds (for a proof see Feng *et al.* [2]):

$$\left(1 - (1 + \alpha_i)\frac{m_i}{r_i}\right)K_i - a_{ij}\left(1 - \frac{m_j}{r_j}\right)K_j > 0, \qquad i, j = 1, 2,\ i \neq j. \tag{2.13}$$

The condition (2.13) also can be expressed in terms of the carrying capacities as

$$K_i > f_i(K_j), \qquad i = 1, 2,\ i \neq j, \tag{2.14}$$

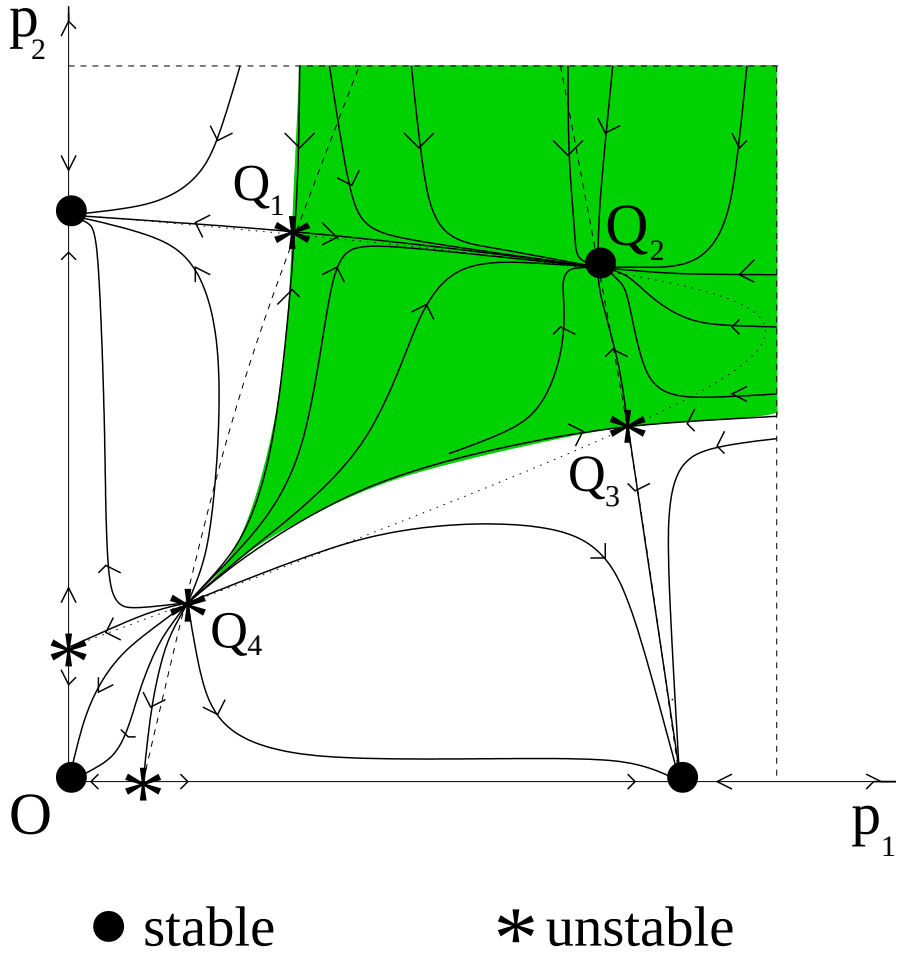

Figure 1: There are nine possible non-trivial equilibria even when $\lambda_i < 1$, $i = 1, 2$.

Table 1: Possible existence of stable equilibria as λ_i and m_i vari. $\Delta > 0$ is assumed for all cases (see the text). BQ_i denotes (stable) boundary equilibrium on the p_i axis and IE denotes (stable) interior equilibrium. Q_0 denotes the trivial equilibrium $(0, 0)$.

	$\lambda_1 \geq 1$	$\lambda_1 < 1,\ K_1 > f_1(K_2)$	$\lambda_1 < 1,\ K_1 < f_1(K_2)$
$\lambda_2 \geq 1$	$BQ_1,\ BQ_2,\ IQ$	$BQ_1,\ BQ_2,\ IQ$	BQ_2
$\lambda_2 < 1,\ K_2 > f_2(K_1)$	$BQ_1,\ BQ_2,\ IQ$	$BQ_1,\ BQ_2,\ IQ$	BQ_2
$\lambda_2 < 1,\ K_2 < f_2(K_1)$	BQ_1	BQ_1	Q_0

where

$$f_i(K_j) = \frac{a_{ij}\left(1 - \frac{m_j}{r_j}\right)K_j}{1 - (1 + \alpha_i)\frac{m_i}{r_i}}, \qquad i, j = 1, 2,\ i \neq j. \tag{2.15}$$

Although a coexistence equilibrium cannot exist under the conditions (2.11) and (2.14), stable non-trivial boundary equilibria (competitive exclusion) may exist when (2.14) holds for only one value of i. If (2.14) holds for both $i = 1$ and $i = 2$, then neither non-trivial boundary nor interior equilibria are possible, i.e., both species will go extinct. Detailed mathematical proofs of these results are provided by Feng *et al.* [2]). A stable interior equilibrium is possible when

$$\lambda_1 \geq 1 \qquad \text{and} \qquad \lambda_2 \geq 1, \tag{2.16}$$

or when

$$\lambda_i \geq 1, \quad \lambda_j < 1, \quad K_j > f_j(K_i), \qquad i, j = 1, 2, \quad i \neq j. \tag{2.17}$$

The condition (2.16) implies that the modified colonization rate of both species exceeds their respective extinction rate. The condition (2.17) states that only one species' colonization rate exceeds its extinction rate, but the other species has a carrying capacity that is above the threshold given by (2.15). Stabilities of various equilibria can be described in terms of λ_i, K_i, and the discriminant, Δ, of a fourth degree polynomial whose positive roots determine the property of interior equilibria, i.e., a stable interior equilibrium exists if and only if $\Delta > 0$. (This polynomial is extremely complex and will not be discussed here–see Feng *et al.* [2]) for details). If we assume $\Delta > 0$ (which is satisfied for the parameter values we use for case studies in Section 4), then the dependence of possible stable equilibria on λ_i and K_i is summarized in Table 1. When a stable interior equilibrium exists, it may attract either all solutions with initial values in $\mathbf{D} = \{(p_1, p_2) | 0 < p_1 < 1, 0 < p_2 < 1\}$, or only solutions with initial values in a sub-region in $\mathbf{D}$, in which case an alternative stable (boundary) equilibrium exists.

Lemma 2.1. *The slow system can have up to 4 interior equilibria and totally up to 9 equilibria in* $\mathbf{D} = \{(p_1, p_2) | 0 < p_1 < 1, 0 < p_2 < 1\}$ *for all the choices of positive parameters, and the system does not have any closed orbit. Moreover, when there exists a unique interior equilibrium, its attracting area is the whole open unit square; and when multiple interior equilibria exist, only one can be stable whose attracting area is only a sub-region of* $\mathbf{D}$*, in which case a stable boundary equilibrium exists.*

Some possible cases for coexistence are listed in Figure 2. We discuss the threshold conditions related to each panel of Figure 2 in the following section.

3 The region of stable coexistence

The following notation will be used in this section:

$$
\begin{aligned}
k_i &= a_{ij}\hat{\beta}_i K_j \alpha_i \alpha_j m_i \frac{m_j}{r_j},\\
\gamma_i &= \frac{1}{a_{ij}\alpha_j K_j \frac{m_j}{r_j}},\\
k_{i0} &= K_i\big(1-\frac{m_i}{r_i}\big) - a_{ij}K_j\big(1-\frac{m_j}{r_j}\big), \qquad i,j=1,2,\ i\neq j.\\
k_{i1} &= K_i\alpha_i\frac{m_i}{r_i},\\
k_{i2} &= \frac{\hat{e}_i(1-a_{12}a_{21})}{\alpha_i\hat{\beta}_i m_i}.
\end{aligned}
\tag{3.1}
$$

For convenience we rewrite the slow system (2.8), with N_i^* replaced by (2.7), as:

$$
p_i' = k_i p_i(1-p_i)\left(-p_j + h_i(p_i)\right), \qquad i,j=1,2, \qquad i\neq j, \tag{3.2}
$$

where

$$
h_i(p_i) = \gamma_i\big(k_{i0} + k_{i1}p_i - \frac{k_{i2}}{1-p_i}\big). \tag{3.3}
$$

The interior equilibria are the intersections of the two isoclines $p_2 = h_1(p_1)$ and $p_1 = h_2(p_2)$. These two isoclines are hyperbolas with two branches and have $p_1 = 1$ and $p_2 = 1$ as a vertical and horizontal asymptote, respectively. Figure 3 depicts one of the possible cases in which there are four interior equilibria (intersections of the two curves) and only Q_2 is stable. The number of interior equilibria may decrease to three, two, and one if parameter values are changed (see Figure 2). As the number of interior equilibria changes, the existence and stability of boundary equilibria also may change, and so is the attraction region of Q_2, which is directly related to the likelihood of coexistence.

It is clear from Figure 2 that the attraction region of Q_2 is reduced when an alternative stable (boundary) equilibrium exists. Next, we choose the parameter values such that two stable non-trivial equilibria are possible with one interior and the other on the p_1 axis (a similar analysis can be performed if p_1 is replaced by p_2). This leads to the following necessary inequalities: **A1.** $K_1 < K_2$, $a_{12} > a_{21}$, $m_1 \geq m_2$, $r_1 > r_2$, $\alpha_1 \leq \alpha_2$, $\hat{\beta}_1 \geq \hat{\beta}_2$. We will fix all parameters except K_2 and $\hat{e}_2$, which will be our bifurcation parameters. Let

$$
K_{2max} = \frac{K_1(1-\frac{m_1}{r_1}) - \dfrac{\hat{e}_1(1-a_{12}a_{21})}{\alpha_1\hat{\beta}_1 m_1}}{a_{12}\left[1-(1-\alpha_2)\frac{m_2}{r_2}\right]}. \tag{3.4}
$$

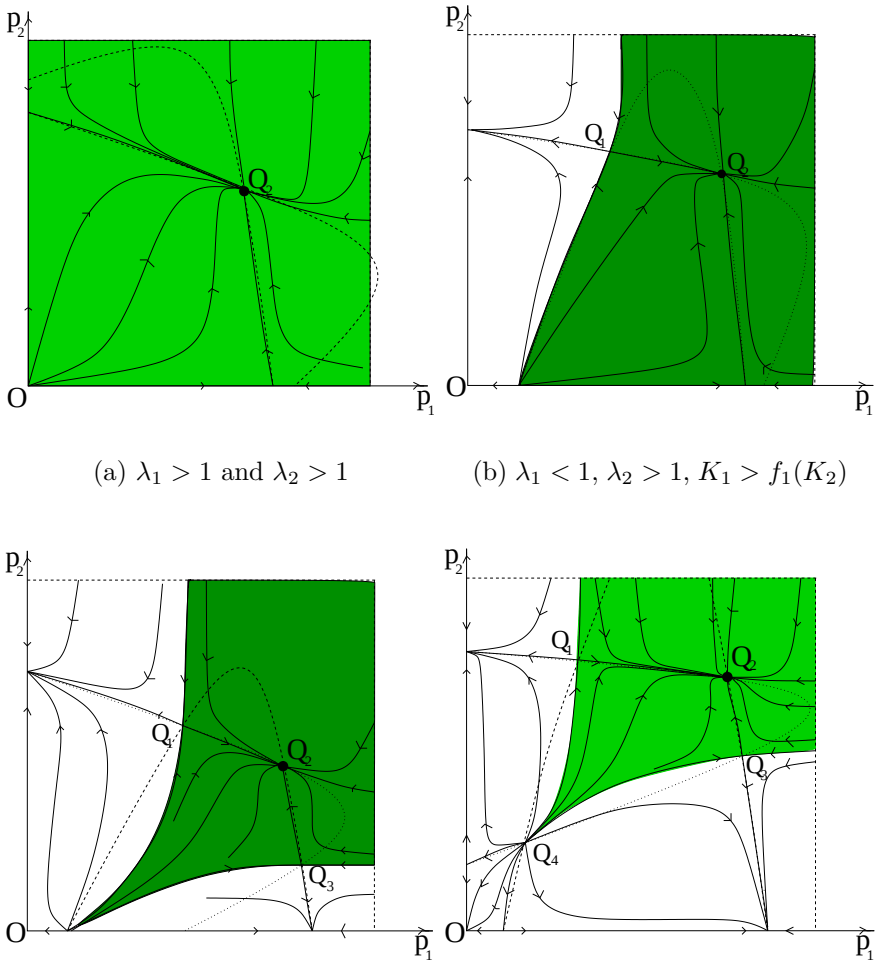

(a) $\lambda_1 > 1$ and $\lambda_2 > 1$

(b) $\lambda_1 < 1$, $\lambda_2 > 1$, $K_1 > f_1(K_2)$

(c) $\lambda_1 < 1$, $\lambda_2 > 1$, $K_1 > f_1(K_2)$

(d) $\lambda_i < 1$, $K_i > f_i(K_j)$, $i, j = 1, 2, i \neq j$

Figure 2: Selected scenarios in which a stable coexistence equilibrium exists. In (a), there is a unique interior equilibrium that attracts all solutions. In (b), there are two interior equilibria, one of which is stable. There also is a stable boundary equilibrium on the p_2 axis. In (c), there are three interior equilibria, one of which is stable, and stable boundary equilibria occur on both the p_1 and the p_2 axes. In (d), there are four interior equilibria, one of which is stable. The trivial equilibrium is also stable.

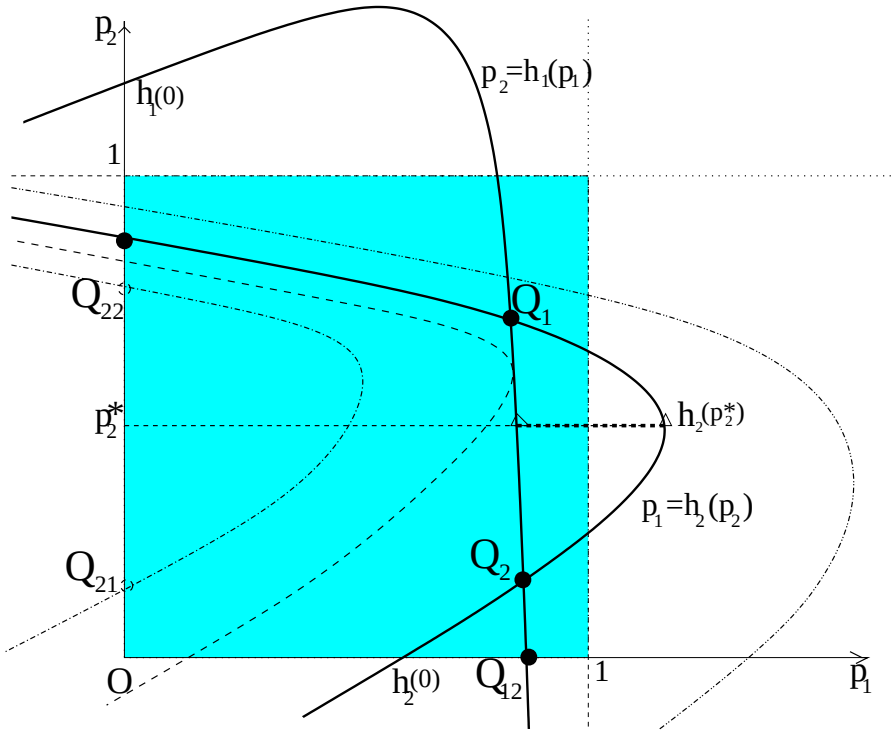

Figure 3: The isoclines of the slow system, boundary and interior equilibria

Then we can verify that $K_2 < K_{2max}$ implies $h_1(0) > 0$. In this case, as shown in Figure 3, the isocline $p_2 = h_1(p_1)$ and the p_1 axis share a unique intersection at $Q_{12} = (p_{12}, 0)$ with $p_{12} \in (0, 1)$, which is the unique nontrivial boundary equilibrium on the p_1 axis. Thus, in the rest of this section we assume that

A2. $0 < K_2 < K_{2max}$.

From the results in Feng *et al.* [2], we know that Q_{10} moves towards the origin as K_2 increases (subject to the constraint $K_2 < K_{2max}$), and that the slow system has at most two interior equilibria for $K_2 \in (0, K_{2max})$.

Next we discuss how the equilibria and their stabilities change with K_2 and $\hat{e}_2$. Notice that an equilibrium on the p_2-axis satisfies $h_2(p_2) = 0$, or equivalently,

$$k_{21}p_2^2 + (k_{20} - k_{21})p_2 + k_{22} - k_{20} = 0. \tag{3.5}$$

Let

$$\begin{aligned} \Delta_2 &= (k_{20} - k_{21})^2 - 4k_{21}(k_{22} - k_{20}) \\ &= \left[-a_{21}K_1\big(1 - \frac{m_1}{r_1}\big) + K_2\big(1 - (1+\alpha_1)\frac{m_2}{r_2}\big)\right]^2 - \frac{4\hat{e}_2(1 - a_{21}a_{12})}{r_2\hat{\beta}_2}K_2. \end{aligned}$$

Then the equation (3.5) has either two solutions if $\Delta_2 > 0$ or no solutions if $\Delta_2 < 0$. Solving the quadratic equation $\Delta_2 = 0$ in terms of K_2 we get

$$K_2 = c_{20} + c_{21}\hat{e}_2 + c_{21}\sqrt{\hat{e}_2^2 + c_{22}\hat{e}_2}, \tag{3.6}$$

where

$$\begin{aligned} c_{20} &= \frac{a_{21}K_1(1-\frac{m_1}{r_1})}{1-(1-\alpha_2)\frac{m_2}{r_2}}, \\ c_{21} &= \frac{2(1-a_{12}a_{21})}{r_2\hat{\beta}_2[1-(1-\alpha_2)\frac{m_2}{r_2}]^2}, \\ c_{22} &= \frac{r_2\hat{\beta}_2 a_{21}K_1(1-\frac{m_1}{r_1})[1-(1-\alpha_2)\frac{m_2}{r_2}]}{1-a_{12}a_{21}}. \end{aligned}$$

The right hand side of (3.6) defines a function of $\hat{e}_2$, which determines a curve of saddle-node bifurcation. We denote this function by $K_{2sn1}(\hat{e}_2)$ ("sn" for saddle-node bifurcation). Hence, as K_2 increases through K_{2sn1}, a saddle-node bifurcation occurs, and there are two equilibria on the p_2 axis (Figure 3). Denote these two equilibria by $Q_{21} = (0, p_{21})$ and $Q_{22} = (0, p_{22})$, where $0 < p_{21} < p_{22} < 1$ are the two roots of $h_2(0)$ determined by equation (3.5).

As K_2 continues to increase (subject to the constraint $K_2 < K_{2sn1} < K_{2max}$), the isocline $h_2(p_2)$ on the far left (one of the dashed curves in Figure 3) shifts to the right, and when it intersects with the isoclines $p_2 = h_1(p_1)$ the interior equilibria appear (the solid curves). To locate this bifurcation curve, we notice that $h_2(p_2)$ has a local minimum at

$$p_2^* = 1 - \frac{1}{\alpha_2 m_2}\sqrt{\frac{r_2\hat{e}_2(1-a_{12}a_{21})}{\hat{\beta}_2 K_2}}.$$

This allows for another saddle-node bifurcation when $p_2^* = h_1\left(h_2(p_2^*)\right)$, which defines the bifurcation curve

$$K_2 = K_{2sn2}(\hat{e}_2) \tag{3.7}$$

in the positive quadrant (see Figure 3 and Figure 4). Hence, there are no interior equilibria for $0 < K_2 < K_{2sn2}$. As K_2 increases to cross the curve $K_2 = K_{2sn2}$, two equilibria Q_1 and Q_2 appear in the interior of $\mathbf{D}$ through a saddle-node bifurcation. Feng *et al.* [2] show that Q_1 is an attracting node and Q_2 is a saddle point.

Another saddle-node bifurcation occurs when the equilibrium Q_{21} on the p_2 axis moves downward and passes through the origin, which occurs at $h_2(0) = 0$ (Figure 3), or

$$K_2 = K_{2sn3}(\hat{e}_2) = \frac{a_{21}K_1(1-\frac{m_1}{r_1})}{1-\frac{m_2}{r_2}} + \frac{(1-a_{12}a_{21})\hat{e}_2}{\alpha_2\hat{\beta}_2 m_2(1-\frac{m_2}{r_2})}. \tag{3.8}$$

Hence, when K_2 increases and passes K_{2sn3}, the number of nontrivial boundary equilibria on the p_2 axis changes from two to one (Figure 4). An ecological consequence of this change is an increase of the attraction region of the stable coexistence equilibrium.

If K_2 continues to increase, the interior equilibrium Q_2 will coalesce with Q_{12} on the p_1 axis and move out of the region $\mathbf{D}$ through another saddle-node bifurcation. The bifurcation curve is determined by $h_1(h_2(0)) = 0$. Solving this equation for K_2 we get

$$K_2 = K_{2sn4}(\hat{e}_2) = d_{20} + d_{21}\hat{e}_2 + d_{22}\sqrt{\hat{e}_2^2 + d_{23}\hat{e}_2 + d_{24}} \tag{3.9}$$

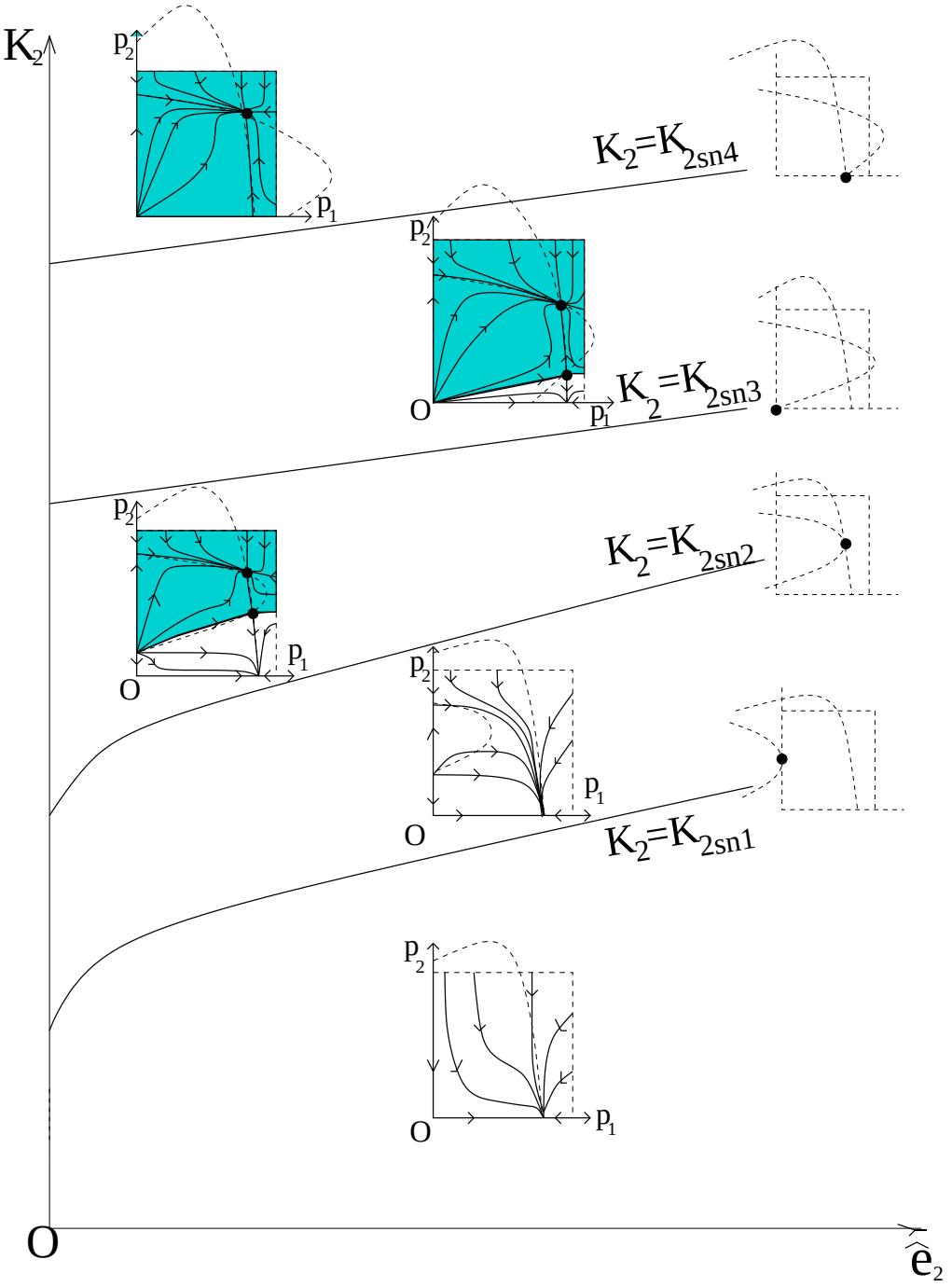

Figure 4: Bifurcation diagram using $\hat{e}_2$ and K_2 as parameters

where

$$
\begin{aligned}
d_{20} &= \frac{a_{21}K_1[1-(1-\alpha_1)\frac{m_1}{r_1}]}{2(1-\frac{m_2}{r_2})},\\
d_{21} &= \frac{1-\frac{1}{2}a_{12}a_{21}}{\alpha_2\hat{\beta}_2 m_2(1-\frac{m_2}{r_2})},\\
d_{22} &= \frac{a_{12}a_{21}}{2\alpha_2\hat{\beta}_2 m_2(1-\frac{m_2}{r_2})},\\
d_{23} &= -\frac{2}{a_{12}}K_1\alpha_2\hat{\beta}_2 m_2[1-(1-\alpha_1)\frac{m_1}{r_1}],\\
d_{24} &= \frac{(\alpha_2\hat{\beta}_2 m_2)^2}{r_1\hat{\beta}_1 a_{12}^2}\left[r_1\hat{\beta}_1(1-(1-\alpha_2)\frac{m_2}{r_2})^2K_1^2-4\hat{e}_1K_1\right].
\end{aligned}
$$

When K_2 increases and passes K_{2sn4}, the number of nontrivial interior equilibria changes from two to one and the attraction region of the stable coexistence equilibrium gets further increased.

Finally, for $K_{2sn4} < K_2 < K_{2max}$, the slow system has a unique interior equilibria Q_1 that is attracting (Figure 4).

We summarize the above results in the following theorem and in Figure 4.

Theorem 3.1. *Assume* **A1** *and* **A2**. *For any fixed* $\hat{e}_2 > 0$ *and* $K_2 \in (0, K_{2max})$, *the slow system (*3.2*) undergoes four saddle-node bifurcations along the curves in the* $(\hat{e}_2, K_2)$ *plane: (i)* $K_2 = K_{2sn1}(\hat{e}_2)$ *is unstable and the bifurcation occurs on the* p_2*-axis; (ii)* $K_2 = K_{2sn2}(\hat{e}_2)$ *is stable and the bifurcation occurs in the interior of* $\mathbf{D}$*; (iii)* $K_2 = K_{2sn3}(\hat{e}_2)$ *is unstable and the bifurcation occurs at the origin; and (iv)* $K_2 = K_{2sn4}(\hat{e}_2)$ *is stable and the bifurcation occurs on the* p_1*-axis. Moreover, the system (*3.2*) has*

(a) a unique stable boundary equilibrium, Q_{12}, *on the* p_1*-axis for* $0 < K_2 < K_{2sn1}$;

(b) two boundary equilibria, Q_{21} *and* Q_{22}, *on the* p_2*-axis for* $K_{2sn1} < K_2 < K_{2sn2}$, *with* Q_{22} *being a saddle and* Q_{21} *being a repelling node;*

(c) two interior equilibria, Q_1 *and* Q_2, *for* $K_{2sn2} < K_2 < K_{2sn3}$, *with* Q_1 *being a stable node and* Q_2 *being a saddle point;*

(d) two interior equilibria as in (c) and two boundary equilibria, Q_{12} *and* Q_{22}, *for* $K_{2sn3} < K_2 < K_{2sn4}$, *with* Q_{12} *being a stable node and* Q_{22} *being a saddle point;*

(e) a unique attracting interior equilibria, Q_1, *and two boundary equilibria,* Q_{12} *and* Q_{22}, *for* $K_{2sn4} < K_2 < K_{2max}$, *with both boundary equilibria being saddle points.*

4 Case study

The results in Theorem 3.1 can provide useful insights into ecological consequences resulting from changes in parameters governing the system. As an example, we consider

Table 2: The bifurcation values for the four cases

	Case 1: $\hat{e}_2 = 4$	**Case 2**: $\hat{e}_2 = 2.5$	**Case 3**: $\hat{e}_2 = 1$	**Case 4**: $\hat{e}_2 = 0.2$
K_{2max}	223.40	340.29	696.12	7011.95
K_{2sn4}	91.09	81.27	99.36	838.87
K_{2sn3}	89.05	78.15	92.98	774.60
K_{2sn2}	86.19	72.18	71.46	416.01
K_{2sn1}	84.57	69.93	67.66	385.44

the potential dynamics of two species of rodents, *Peromyscus leucopus* and *Tamias striatus*, that occupy remnant forest patches in the central United States. Our studies of the species in Indiana have revealed that they rely upon a common core food resource (Ivan and Swihart [12]; Swihart et al. [27]) and exhibit weak levels of competition in which *T. striatus* is dominant (Nupp and Swihart [26]). However, *T. striatus* is more sensitive to the effects of forest fragmentation than *P. leucopus* and typically occurs at lower densities (Henein et al. [9]; Nupp and Swihart [19]). Thus, this system can provide a useful illustration of the potential effects of varying levels of habitat loss and extinction risk on the outcome of competition.

Using our knowledge of this system, we assigned the following set of realistic parameter values to observe numerically (using MAPLE) the quantitative changes to the attracting region of the stable coexistence equilibrium. In all that follows, species 1 is the inferior competitor (*Peromyscus leucopus*) and species 2 is the superior competitor (*Tamias striatus*):

$$\begin{array}{llll} r_1 = 0.7, & m_1 = 0.1, & \alpha_1 = 0.5, & \beta_1 = 0.05, \\ r_2 = 0.15, & m_2 = 0.1, & \alpha_2 = 0.6, & \beta_2 = 0.03, \\ a_{12} = 0.5, & a_{21} = 0.1 & & \end{array} \tag{4.1}$$

Note that the relative locations of the bifurcation curves described in Theorem 3.1 are dependent on other parameter values, including K_1 and $\hat{e}_1$. We considered four cases corresponding to the following four sets of K_1 and $\hat{e}_1$:

Case 1. $K_1 = 100$ and $e_1 = 0.01$;

Case 2. $K_1 = 150$ and $e_1 = 0.01$;

Case 3. $K_1 = 300$ and $e_1 = 0.005$;

Case 4. $K_1 = 3000$ and $e_1 = 0.001$.

These cases correspond to decreasing severity of habitat fragmentation and extinction risk. In many parts of the midwestern United States, a carrying capacity of 100 for *P. leucopus* (Case 1.) represents a situation in which each forest remnant is only 0.1-3 ha in size (Nupp and Swihart [18]). Density of *P. leucopus* declines nonlinearly as forest patch area increases (Nupp and Swihart [18], [20]), with the result that average patch sizes for Cases 2-4 are roughly 3-5 ha, 10-20 ha, and 100-300 ha, respectively.

The bifurcation curves for all four cases were computed using MAPLE and are shown in Figure 5. Clearly, the mouse-chipmunk system shows the same qualitative properties

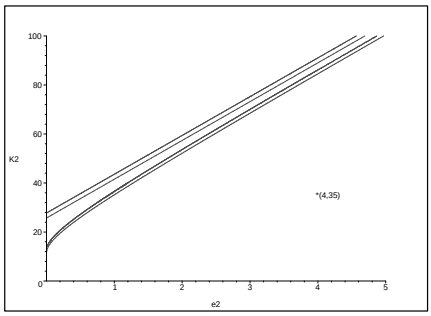

(a) case 1: $K_1 = 100, \hat{e}_1 = 1$

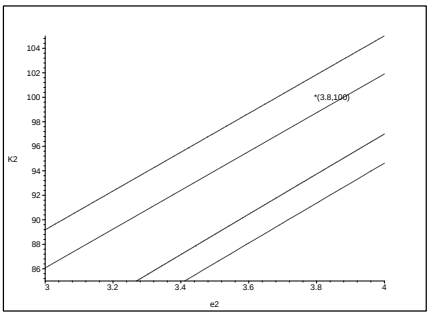

(b) case 2: $K_1 = 150, \hat{e}_1 = 1$

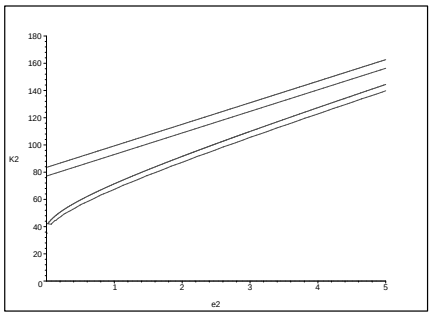

(c) case 3: $K_1 = 300, \hat{e}_1 = 0.5$

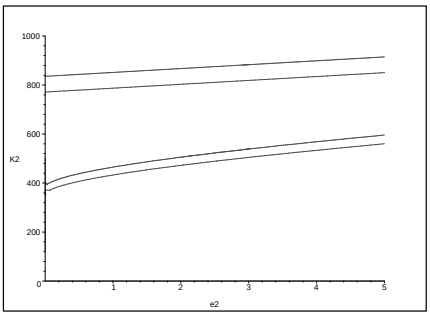

(d) case 4: $K_1 = 3000, \hat{e}_1 = 0.1$

Figure 5: Bifurcation diagram for the four cases.

as that in Fig 4. Several points on the bifurcation curves are listed in Table 2. For example, if $K_1 = 300$, $e_1 = 0.005$ (case 3) and $\hat{e}_2 = 1$ (or $e_2 = 0.01$), then $K_{2sn4} = 99$, $K_{2sn2} = 72$. Hence, according to Theorem 3.1, for $K_2 > 99$, the attracting region of the stable interior equilibrium is the entire interior of $\mathbf{D}$ (coexistence is expected for all initial data), whereas for $72 < K_2 < 99$, there exists a stable boundary equilibrium on the p_1 axis which attracts solutions with initial data in the unshaded part of $\mathbf{D}$ (competitive exclusion of species 2). For $K_2 < 72$, coexistence is impossible and species 2 will always suffer extinction, despite its competitive superiority. A notable pattern from this example is the narrow range over which coexistence thresholds occur when carrying capacity (and hence forest patch size) is small. In highly fragmented landscapes characterized by small patches with low carrying capacities, slight changes in K_2 or e_2 can make the difference between coexistence and competitive exclusion. For *T. striatus*, local carrying capacities are approximately 35, 100, 225, and 3000 for Cases 1-4, respectively (Nupp and Swihart [19]). Thus, competitive coexistence becomes increasingly likely as forest patch size increases. We do not have reliable estimates for background extinction rates in this system, but the values used in Table 2 are illustrative of the process. For a landscape, with extremely small patches (Case 1), *T. striatus* is predicted to suffer extinction despite its competitive advantage. A slight increase in patch size (Case 2) may lead to stable coexistence, albeit in a subset of the interior of $\mathbf{D}$ (Figure 5). For large patches with correspondingly large carrying capacities, stable coexistence is predicted for all occupancy levels (Figure 5).

5 Conclusions

Our model demonstrates the importance of considering local patch dynamics when attempting to understand the behavior of metacommunities structured partly by competition. A focus solely on colonization and extinction processes fails to capture the rich dynamics associated with systems that are affected by weak competition. Moreover, the interplay between local and landscape-level processes can lead to counter-intuitive results and multiple stable equilibria not predicted by models that ignore either colonization dynamics or competitive interactions. Conservation considerations in fragmented landscapes frequently fail to consider the influence of interspecific interactions on persistence Our model results suggest that failure to account for competitive interactions may lead to biased predictions regarding persistence of species, and these considerations may be especially important as habitat loss and fragmentation intensify.

For decades, competition was touted by ecologists as a dominant force structuring local communities (reviewed by Schluter and Ricklefs [22]). More recently, the role of spatial structure has been increasingly acknowledged as an important predictor of local community structure in fragmented landscapes (e.g., Harrison [8], Wilson [30]). By considering jointly the effects of competition and spatial structure within the context of analytical models such as the one developed in this paper, ecologists may be empowered with the tools needed for a more complete understanding of communities in complex landscapes.

References

[1] Bascompte, J. and R. V. Sole (1998). Effects of habitat destruction in a prey-predator metapopulation model. J. Theor. Biol. 195:383-393.

[2] Feng, Z-L., Y-F. Yi and H-P. Zhu (2003). Metapopulation Dynamics with migration and local competition. Fields Institute Communication, AMS (to appear).

[3] Fenichel, N (1979). Geometric singular perturbation theory for ordinary differential equations. J. Diff. Eqn. 31:53-98.

[4] Gaines, M. S., J. E. Diffendorfer, R. H. Tamarin and T. S. Whittam (1997). The effects of habitat fragmentation on the genetic structure of small mammal populations. Journal of Heredity 88:294-304.

[5] Hanski, I (1998). Metapopulation dynamics. Nature 396:41-49.

[6] Hanski, I (1999). Metapopulation ecology. Oxford University Press.

[7] Hanski, I. and D. Zhang (1993). Migration, metapopulation dynamics and fugitive co-existence. J. Theor. Biol. 163:491-504.

[8] Harrison, S. (1999). Local and regional diversity in a patchy landscape: Native, alien, and endemic herbs on serpentine. Ecology 80:70-80.

[9] Henein, K., J. Wegner and G. Merriam (1998). Population effects of landscape model manipulation on two behaviourally different woodland small mammals. Oikos 81:168-186.

[10] Holmes, E. E. and H. B. Wilson (1998). Running from trouble: long-distance dispersal and the competitive coexistence of inferior species. American Naturalist 151:578-586.

[11] Hopf, F. A., T. J. Valone and J. H. Brown (1993). Competition theory and the structure of ecological communities. Evolutionary Ecology 7:142-154.

[12] Ivan, J. S., and R. K. Swihart (2000). Selection of mast by granivorous rodents of the central hardwood forest region. Journal of Mammalogy 81:549-562.

[13] Levins, R (1969). Some demographic and genetic consequences of environmental heterogeneity for biological control. Bull. Entom. Soc. Am. 15:237-240.

[14] O'Malley, R. E. Jr (1974). Introduction to singular perturbations. Academic Press, New York.

[15] McIntosh, R. P (1995). H. A. Gleason's 'individualistic concept' and theory of animal communities: a continuing controversy. Biological Review 70:317-357.

[16] Moilanen, A. and I. Hanski (1995). Habitat destruction and coexistence of competitors in a spatially realistic metapopulation Journal of Animal Ecology 64:141-144.

[17] Nee, S. and R. M. May (1992). Dynamics of metapopulations: habitat destruction and competitive coexistence. Journal of Animal Ecology 61:37-40.

[18] Nupp, T. E. and R. K. Swihart (1996). Effect of forest patch area on population attributes of white-footed mice (Peromyscus leucopus) in fragmented landscapes. Canadian Journal of Zoology 74:467-472.

[19] Nupp, T. E. and R. K. Swihart (1998). Influence of forest fragmentation on population attributes of white-footed mice and eastern chipmunks. Journal of Mammalogy 79:1234-1243.

[20] Nupp, T. E. and R. K. Swihart (2000). Landscape-level correlates of small mammal assemblages in forest fragments of farmland. Journal of Mammalogy 81:512-526.

[21] Nupp, T. E. and R. K. Swihart (2001). Assessing competition between forest rodents in a fragmented landscape of midwestern USA. Mammalian Biology 66:345-356.

[22] Schluter, D. and R. E. Ricklefs (1993). Species diversity: an introduction to the problem. Pages 1-10 in R. E. Ricklefs and D. Schluter (editors), Species diversity in ecological communities. Historical and geographical perspectives. University of Chicago Press, Chicago.

[23] Schoener, T. W (1983). Field experiments on interspecific competition. American Naturalist 122:240-285.

[24] Sheperd, B. F. and R. K. Swihart (1995). Spatial dynamics of fox squirrels (Sciurus niger) in fragmented landscapes. Canadian Journal of Zoology 73:2098-2105.

[25] Slatkin, M (1974). Competition and regional coexistence. Ecology 55:128-134.

[26] Swihart, R. K., Z. Feng, N. S. Slade, D. M. Doran and T. M. Gehring (2001). Effects of habitat destruction and resource supplementation in a predator-prey metapopulation model. J. Theor. Biol. 210:287-303.

[27] Swihart, R. K., T. M. Gehring, M. B. Kolozsvary and T. E. Nupp (2003). Responses of resistant vertebrates to habitat loss and fragmentation: the importance of niche breadth and range boundaries. Diversity and Distributions 9:1-18.

[28] Taneyhill, D. E (2000). Metapopulation dynamics of multiple species: the geometry of competition in a fragmented habitat. Ecological Monographs 70:495-516.

[29] Wang, Z-L., F-Z Wang, S. Chen and M-Y. Zhu (2002). Competition and coexistence in regional habitats. American Naturalist 159:498-508.

[30] Wilson, D. S. (1992). Complex interactions in metacommunities, with implications for biodiversity and higher levels of selection. Ecology 73:1984-2000.

[31] Wilcox, B. A. and D. D. Murphy (1985). Conservation strategy: the effects of fragmentation on extinction. American Naturalist 125:879-887.

[32] Wright, D. H., B. D. Patterson, G. M. Mikkelson, A. Cutler and W. Atmar (1998). A comparative analysis of nested subset patterns of species composition. Oecologia 113:1-20.

[33] Zollner, P. A (2000). Comparing the landscape level perceptual abilities of forest sciurids in fragmented agricultural landscapes. Landscape Ecology 15:523-533.